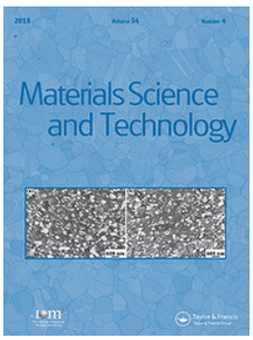

Materials Science and Technology

ISSN: 0267-0836 (Print) 1743-2847 (Online) Journal homepage: https://www.tandfonline.com/loi/ymst20

# Influence of cryogenic thermal treatment on mechanical properties of an Al–Cu–Mg alloy

M. Araghchi, H. Mansouri & R. Vafaei

**To cite this article:** M. Araghchi, H. Mansouri & R. Vafaei (2018) Influence of cryogenic thermal treatment on mechanical properties of an Al–Cu–Mg alloy, Materials Science and Technology, 34:4, 468-472, DOI: 10.1080/02670836.2017.1407553

**To link to this article:** https://doi.org/10.1080/02670836.2017.1407553

MATERIALS SCIENCE AND TECHNOLOGY, 2018
VOL. 34, NO. 4, 468–472
https://doi.org/10.1080/02670836.2017.1407553

The Institute of Materials, Minerals and Mining

Taylor & Francis
Taylor & Francis Group



# Influence of cryogenic thermal treatment on mechanical properties of an Al–Cu–Mg alloy

M. Araghchi, H. Mansouri and R. Vafaei

Department of Materials Engineering, Malek Ashtar University of Technology, Isfahan, Iran

**ABSTRACT**

In this study, a cryogenic thermal treatment is developed and its effects on mechanical properties and precipitates are investigated. Water-quenched samples were immersed in liquid nitrogen and reheated in hot oil at 180°C or boiling water for 5 min. Finally, the samples were artificially aged at 190°C for 12 h. The results indicated a notable increase of about 75 MPa in the ultimate tensile strength in comparison to T6 heat-treated alloy. TEM observations revealed that the S(S′) precipitates were fine and uniformly distributed in the microstructure due to reheating in hot oil and subsequent aging treatment.

**ARTICLE HISTORY**
Received 30 May 2017
Revised 23 October 2017
Accepted 27 October 2017

**KEYWORDS**
Al–Cu–Mg alloy; cryogenic thermal treatment; mechanical properties; TEM evaluations

## Introduction

Deep cryogenic treatment is an important supplementary process of conventional heat treatment to improve the mechanical properties of ferrous and nonferrous metals, such as wear resistance, durability and dimensional stability [1–3]. The use of cryogenic treatment on metallic alloys has grown during the last decades. Most of the investigators in the field of cryogenic treatment have focused on steels, especially tool steels [4–6]. Recently, there has been a great interest in the application of low-temperature heat treatment on nonferrous alloys in order to improve their properties [7–9].

Aluminium alloys are widely used materials in the aerospace industry due to their desirable properties, such as low density, high specific strength and elastic modulus, good corrosion resistance, excellent cryogenic properties and low fatigue crack growth rate [10–12]. The application of cryogenic treatment on aluminium alloys has not received enough attention so far. Some studies have been devoted to investigating the effect of deep cryogenic treatment at −196°C on the properties of aluminium [13–14]. It has been shown that the process used for tool steels cannot be effective for aluminium alloys. For example, Lulay et al. [15] proved cryogenic treatment does not affect strength, hardness and toughness of a 7075-T6 aluminium alloy. In another work, Chen et al. [16] showed that the increase in tensile strength and hardness of an aluminium alloy subjected to deep cryogenic treatment is negligible.

The present work is aimed at studying the possibility of employing a new cryogenic thermal treatment to enhance the mechanical properties of a 2024 aluminium alloy, the most common group of Al–Cu–Mg alloys, and investigate its influence on microstructure.

## Experimental procedures

Samples with dimensions of 55 mm × 25 mm × 25 mm were cut from an as-received extruded billet of a 2024-T3 aluminium alloy. The chemical composition of the alloy is given in Table 1. The samples were solution treated by heating to 495 ± 5°C for 2 h and then quenched in water at 20°C. Subsequently, the samples were reheated in hot oil or boiling water after cryogenic treatment through immersion in liquid nitrogen for 24 h. Finally, these samples were artificially aged at 190 ± 6°C for 12 h. For comparison, T4 and T6 heat-treated samples were also provided. The detailed descriptions along with sample label are given in Table 2. Figure 1 illustrates the schematic of cryogenic thermal treatment cycles used in this study.

Tensile specimens were cut from the heat-treated samples using the electric discharge machining (EDM) method with the dimensions in accordance with the standard of ASTM E8-13. Uniaxial tensile tests were carried out with a 5 kN tensile machine which utilised a laser extensometer at room temperature. Uncertainties in the 0.2% yield stress and tensile strength were ±4% and ±2%, respectively. Three samples were tested for each condition and the average values were reported. The measurement of the Rockwell B hardness was carried out in accordance with ASTM E18-13. For each sample, at least five points were measured and the average value obtained was recorded with a typical uncertainty of ±1%. Schematic of the locations of the tensile

**CONTACT** H. Mansouri hoj.mansouri@gmail.com; M. Araghchi m.araghchi@gmail.com

**Table 1.** Chemical compositions of 2024 aluminium alloy (wt-%).

| Element | Cu | Mg | Mn | Si | Fe | Cr | Zn | Ti | Al |
|---|---|---|---|---|---|---|---|---|---|
| Nominal | 3.8–4.9 | 1.2–1.8 | 0.3–0.9 | < 0.5 | < 0.5 | < 0.1 | < 0.25 | < 0.15 | Bal. |
| In this study | 4.37 | 1.29 | 0.6 | 0.3 | 0.4 | 0.052 | 0.075 | 0.009 | Bal. |

test specimens and hardness measurement is given in Figure 2.

Disc-shaped specimens, 5 mm in diameter and 1 mm thick, were punched from the slices cut from the samples by EDM. Differential scanning calorimetry (DSC) measurements were carried out on a PERKIN-ELMER Pyris-1 apparatus, scanning from room temperature to 500°C at a heating rate of 10°C $min^{-1}$. An empty aluminium pan was used as a reference. Final data were corrected by subtracting a previously established baseline from a DSC run with empty pans.

A field-emission transmission electron microscope (JEM-2100F TEM) was used to characterise the microstructure of the samples. The TEM specimens were prepared by mechanical grinding and polishing down to about 100 µm and then punched into discs of 3 mm followed by twin-jet polishing using a solution of 25% nitric acid +75% methanol at a temperature maintained between −40°C and −30°C at 20 V. The length distributions of the precipitates were measured based on numerous TEM micrographs and by the use of image analysis software. About 200 precipitates were taken into consideration per each sample.

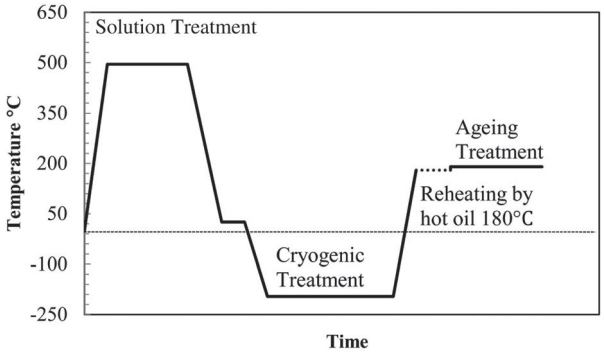


**Figure 1.** Schematic of the cryogenic thermal treatment cycle.

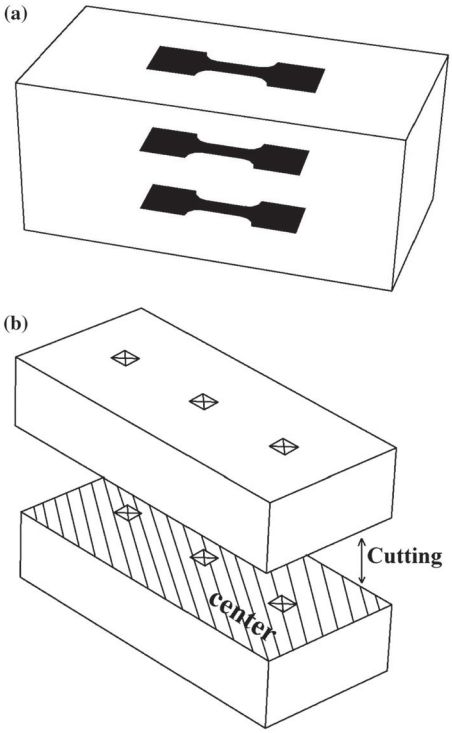


**Figure 2.** Schematic of the locations of (a) the extracted tensile test specimens and (b) hardness measurement.

## Result and discussion

Figure 3 illustrates the engineering stress–strain curves of samples with different treatments. Mechanical properties of the samples are given in Table 3. It can be seen that ultimate tensile strength (UTS) of the T6 sample is 506 MPa. It increased by 14.8% and reaches 581 MPa in the CTTO sample. Furthermore, the yield strengths (YS) of the CTTO sample is 12.5% higher than that of T6 sample.

It should also be mentioned that as compared to the T6 sample, the elongation of the CTTO is slightly reduced about 1.8%, indicating that cryogenically treated sample possess a good combination of strength and ductility. Mechanical behaviour of the CTTB sample shows that UTS and YS have increased by 6.7% and 2.5%, respectively. It is found that the enhancement of the strength is lower as compared with the CTTO sample.

Table 3 shows that the hardness of the T4 and the T6 sample is 74.6 HRB and 79.2 HRB, respectively. It increases to 86.7 HRB for the CTTO sample. Reheating

**Table 2.** Sample identification codes, quenching media and their corresponding condition.

| Sample name | Solution heat treatment | Quenching media | Immersion in liquid nitrogen | Reheating medium | Aging |
|---|---|---|---|---|---|
| T4 | 495°C, 2 h | Water at 20°C | – | – | Natural aging, 30 day |
| T6 | | | – | – | 190°C, 12 h |
| CTTO | | | 24 h | Oil 180°C | |
| CTTB | | | 24 h | Boiling water | |

Note: CTTO: cryogenic thermally treated by hot oil; CTTB: cryogenic thermally treated by boiling water.

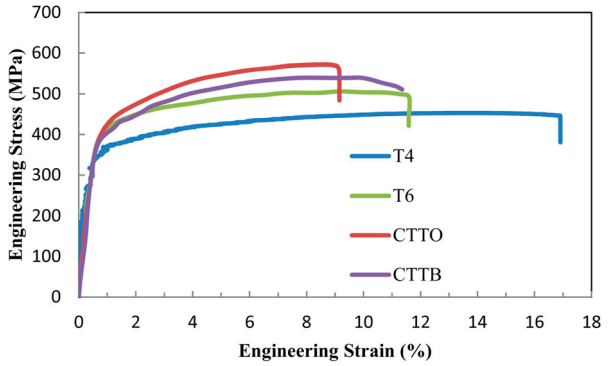


**Figure 3.** The engineering stress–strain curves of 2024 aluminium alloys for different treatments.

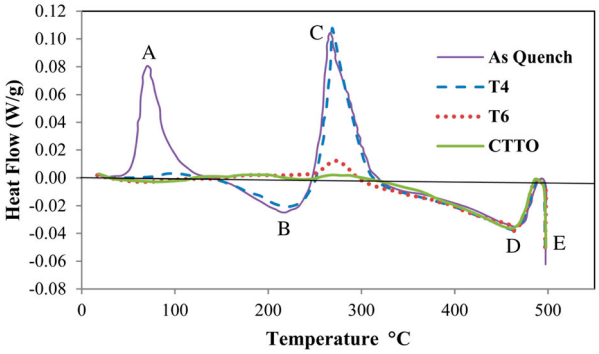


**Figure 4.** DSC curves of 2024 aluminium alloy in different conditions.

**Table 3.** Hardness and tensile properties of the samples for different treatments.

| Sample name | Hardness (HRB) | 0.2% yield stress (MPa) | Ultimate tensile strength (MPa) | Elongation to failure (%) |
|---|---|---|---|---|
| T4 | 74.6 ± 0.8 | 317 ± 12 | 453 ± 9 | 16.3 ± 0.7 |
| T6 | 79.2 ± 0.8 | 358 ± 14 | 506 ± 10 | 11.6 ± 0.4 |
| CTTO | 86.7 ± 0.9 | 403 ± 17 | 581 ± 12 | 9.8 ± 0.3 |
| CTTB | 81.1 ± 0.9 | 367 ± 14 | 540 ± 11 | 11.4 ± 0.4 |

the sample in the hot oil with a temperature close to the aging temperature leads to an increase of hardness from 79.2 HRB to 86.7 HRB. Moreover, the hardness of the sample heat treated in boiling water is 81.1 HRB which shows a slight increase in comparison with the T6 one.

The DSC curves of the 2024 aluminium alloy at different conditions are shown in Figure 4. Five heat effects, marked as A–E, are determined for as-quenched condition. Previous DSC studies [17,18] on Al–Cu–Mg alloys have shown that A and B are exothermic and endothermic effect related to the formation and dissolution of Cu–Mg co-clusters or GPB (Guinier-Preston-Bagaryatsky) zones, respectively. Moreover, the precipitation and dissolution of S(S′) phase can be discernible through C and D. For the water-quenched and naturally aged sample (T4), there is no evidence of peak A, indicating that the formation of the precipitate associated with effect A has completed during long natural aging. Furthermore, the co-existence of the peaks B and C suggests that Cu–Mg co-clusters dissolve and are replaced by the S phase during the artificial aging. It is clearly observed that for the T6 sample, the A and B peaks have disappeared, whereas the peak C is still present. This shows that the formation of the S(S′) precipitates has not completed during artificial aging. The thermogram of the CTTO samples shows that there are no peaks attributed to the formation of the co-clusters and S(S′) phase. Moreover, the area of peak C is almost nil. So, it can be said that the precipitation of S(S′) phase has been accelerated due to an increase in heterogeneous nucleation sites and the absence of GPB zones during cryogenic thermal treatment.

The difference between that strength of the samples can be attributed to their microstructure. TEM micrograph and corresponding SAD patterns taken along the $[100]_{Al}$ zone axis of T6 and CTTO samples are given in Figure 5. Histograms showing the length of precipitates are also included. The formation of big needle-like precipitates with an average size of 270 nm in the T6 sample can be seen. They are determined to be the S(S′) phase which has a significant role in strengthening 2024 aluminium alloy during artificial aging [19,20]. The main precipitates which have been considered in Al–Cu–Mg-base alloys are the S′ or S ($Al_2CuMg$) [21] phase after artificial aging [22]. It has been reported that the crystal structure and chemical composition of the S′ phase are considered identical to the equilibrium S phase [23] (Cmcm, $a = 0.400$ nm, $b = 0.923$ nm and $c = 0.714$ nm) [24] but with varying lattice dimension [25]. As shown by Bagaryatsky [26] and Silcock [27], the orientation relationship between the precipitates and the aluminium matrix is [100]Al // [100]S(S′); [021]Al // [010]S(S′); [012]Al // [001]S(S′). These precipitates are considered to be non-shearable [28,29]. The microstructure and SAD pattern of the CTTO sample show that cryogenic thermal treatment has not changed the type of precipitates [30] but their average size has decreased to 110 nm (Figure 5(b)). So, new cryogenic thermal treatment results in fine and well-distributed precipitates. Moreover, this is why the mechanical properties of CTTO are superior to the other samples.

Cryogenic treatment followed by reheating in hot oil at 180°C results in surface expansion. On the other hand, the core of sample at a lower temperature acts as a barrier. This matter along with the existence of residual stress results in plastic deformation in the CTTO sample [31,32]. Subsequently, dislocation density increases which are the preferred nucleation site for precipitation during artificial aging [33]. It has been proved that dislocation accelerates the kinetics of precipitation hardening in aluminium alloys [23,34]. Therefore, the precipitates become finer and the strength increases. The difference in temperature between the surface and

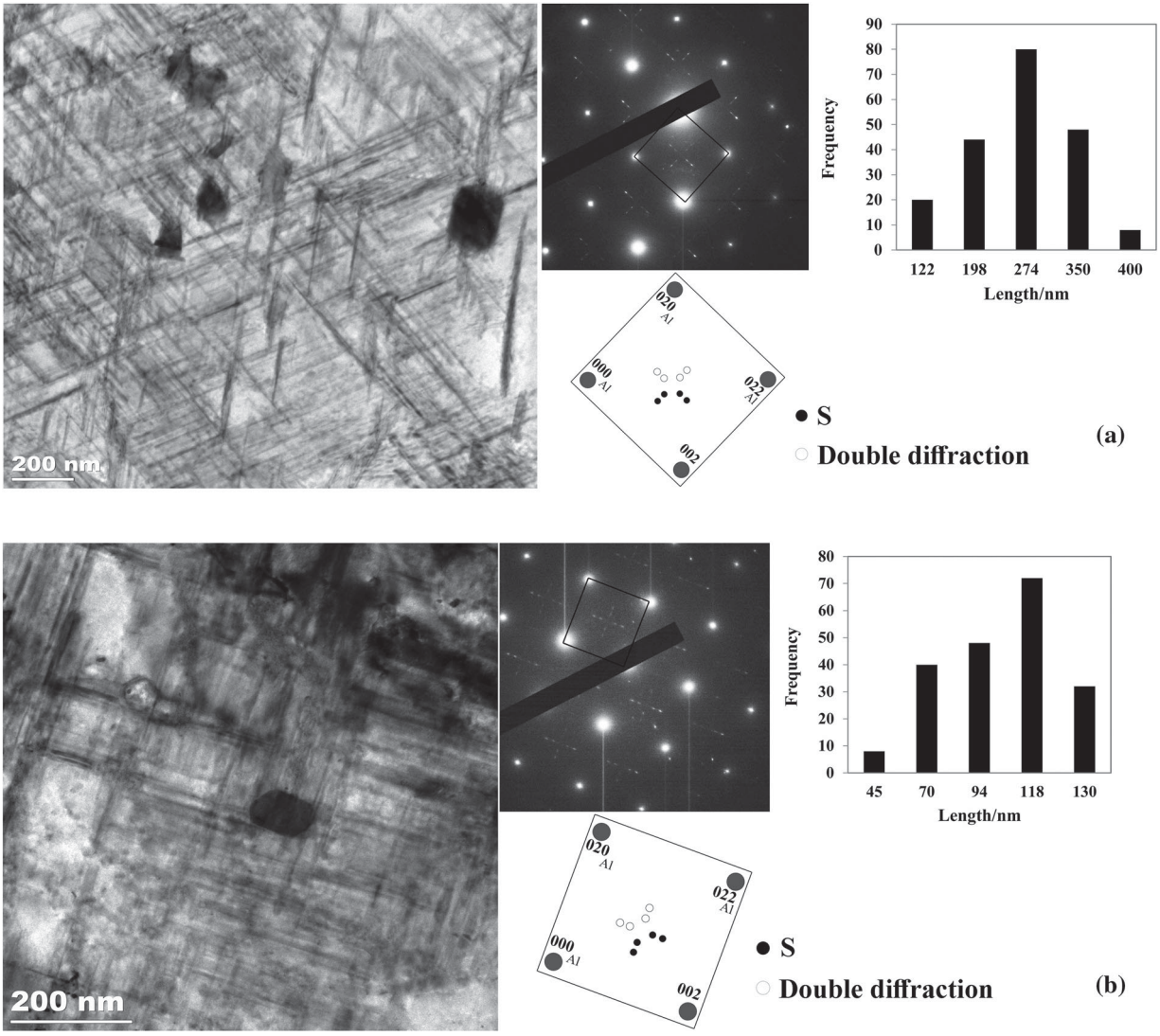


**Figure 5.** TEM image, SAED, simulated diffraction pattern and frequency distribution of the precipitates, (a) T6 and (b) new cryogenically treated sample of 2024 aluminium alloy, $B = [100]_{Al}$.

core of the samples as a result of reheating in boiling water is not much as hot oil. Thus, the enhancement of the strength of the CTTB sample is lower in comparison with the CTTO one.

## Conclusion

In summary, in the present work, a 2024 aluminium alloy underwent new cryogenic thermal treatment. The UTS and hardness of the cryogenic-treated sample increased by about 75 MPa and 8.5 HRB, respectively, as compared with T6 heat-treated temper. The increase in strength did not achieve at the expense of drop in elongation and it reduced just by 1.8%. The DSC thermograms of the CTTO sample indicated that the precipitation of the S(S′) phase has already been completed. Microstructural evolution showed that the S(S′) precipitates in the cryogenically treated sample were fine and well distributed, and this was responsible for the enhancement of mechanical properties.

## Disclosure statement

No potential conflict of interest was reported by the authors.

## References

[1] Wilkins C. Cryogenic processing; the big chill. EDM Today. 1999:36–44.
[2] Ray KK, Das D. Improved wear resistance of steels by cryotreatment: the current state of understanding. Mater Sci Technol. 2017;33(3):340–354.
[3] Siva RS, Jaswin MA, Lal DM. Enhancing the wear resistance of 100Cr6 bearing steel using cryogenic treatment. Tribol Trans. 2012;55(3):387–393.
[4] Gavriljuk V, Theisen W, Sirosh V, et al. Low-temperature martensitic transformation in tool steels in relation to their deep cryogenic treatment. Acta Mater. 2013;61(5):1705–1715.
[5] Kumar TV, Thirumurugan R, Viswanath B. Influence of cryogenic treatment on the metallurgy of ferrous alloys-a review. Mater Manuf Process. 2017;32(16):1789–1805.
[6] Das D, Dutta AK, Ray KK. Inconsistent wear behaviour of cryotreated tool steels: role of mode and mechanism. Mater Sci Technol. 2009;25(10):1249–1257.

[7] Gu K, Zhang H, Zhao B, et al. Effect of cryogenic treatment and aging treatment on the tensile properties and microstructure of Ti–6Al–4V alloy. Mater Sci Eng A. 2013;584:170–176.
[8] Liu Y, Shao S, Xu C-S, et al. Effect of cryogenic treatment on the microstructure and mechanical properties of Mg–1.5 Zn–0.15 Gd magnesium alloy. Mater Sci Eng A. 2013;588:76–81.
[9] Li J, Zhou J, Xu S, et al. Effects of cryogenic treatment on mechanical properties and micro-structures of IN718 super-alloy. Mater Sci Eng A. 2017;707(Suppl C):612–619.
[10] Peel C. Aluminium alloys for airframes–limitations and developments. Mater Sci Technol. 1986;2(12):1169–1175.
[11] Williams JC, Starke EA. Progress in structural materials for aerospace systems. Acta Mater. 2003;51(19):5775–5799.
[12] Immarigeon JP, Holt RT, Koul AK, et al. Lightweight materials for aircraft applications. Mater Charact. 1995;35(1):41–67.
[13] Bouzada F, Cabeza M, Merino P, et al., editors. Effect of deep cryogenic treatment on the microstructure of an aerospace aluminum alloy. Adv Mater Res. 2012;445:965–970.
[14] Li C-M, Cheng N-P, Chen Z-Q, et al. Deep-cryogenic-treatment-induced phase transformation in the Al-Zn-Mg-Cu alloy. Int J Min Met Mater. 2015;22(1):68–77.
[15] Lulay K, Khan K, Chaaya D. The effect of cryogenic treatments on 7075 aluminum alloy. J Mater Eng Perform. 2002;11(5):479–480.
[16] Chen P, Malone T, Bod R, et al. Effects of cryogenic treatment on the residual stress and mechanical properties of an aerospace aluminum alloy. AMPET Conference; 2000 Sep 18–20; Huntsville, AL; United States.
[17] Jena A, Gupta A, Chaturvedi M. A differential scanning calorimetric investigation of precipitation kinetics in the Al-1.53 wt% Cu-0.79 wt% Mg alloy. Acta Metall. 1989;37(3):885–895.
[18] Shih H-C, Ho N-J, Huang J. Precipitation behaviors in Al-Cu-Mg and 2024 aluminum alloys. Metall Mater Trans A. 1996;27(9):2479–2494.
[19] Ringer S, Sakurai T, Polmear I. Origins of hardening in aged Al-Cu-Mg-(Ag) alloys. Acta Matera. 1997;45(9):3731–3744.
[20] Wang S, Starink M, Gao N. Precipitation hardening in Al–Cu–Mg alloys revisited. Scripta Mater. 2006;54(2):287–291.
[21] Radmilovic V, Thomas G, Shiflet G, et al. On the nucleation and growth of Al2CuMg (S′) in Al-Li-Cu-Mg and Al-Cu-Mg alloys. Scripta Metall. 1989;23(7):1141–1146.
[22] Radmilovic V, Kilaas R, Dahmen U, et al. Structure and morphology of S-phase precipitates in aluminum. Acta Mater. 1999;47(15):3987–3997.
[23] Wilson R, Partridge P. The nucleation and growth of S'precipitates in an aluminium-2.5% copper-1.2% magnesium alloy. Acta Metall. 1965;13(12):1321–1327.
[24] Perlitz H, Westgre A. The crystal structure of $Al_2CuMg$. Ark Chemical. 1943;16:1–5.
[25] Kilaas R, Radmilovic V. Structure determination and structure refinement of Al2CuMg precipitates by quantitative high-resolution electron microscopy. Ultramicroscopy. 2001;88(1):63–72.
[26] Bagaryatsky YA, editor. Mechanism of artificial aging of Al-Cu-Mg alloy. Doklady Akad Nauk SSSR. 1952;87:397–400.
[27] Silcock J, Heal T, Hardy H. Structural ageing characteristics of binary aluminium-copper alloys. J Inst Met. 1954;82:239–248.
[28] Starink MJ, Yan J, editors. Precipitation hardening in Al-Cu-Mg alloys: analysis of precipitates, modelling of kinetics, strength predictions. Mater Sci Forum. 2006;519–521:251–258. Trans Tech Publ.
[29] Cahn R, Haasen P. Physical metallurgy. Vol. III. Amsterdam, The Netherlands: Elsevier Science BV; 1996.
[30] Wang S, Starink M. Precipitates and intermetallic phases in precipitation hardening Al–Cu–Mg–(Li) based alloys. Int Mater Rev. 2005;50(4):193–215.
[31] Simencio ECA, Canale LCF, Totten GE. Uphill quenching of aluminium: a process overview. Int Heat Treat Surf Eng. 2011;5(1):26–30.
[32] Lados DA, Apelian D, Wang L. Minimization of residual stress in heat-treated Al–Si–Mg cast alloys using uphill quenching: mechanisms and effects on static and dynamic properties. Mater Sci Eng A. 2010;527(13–14):3159–3165.
[33] Ratchev P, Verlinden B, De Smet P, et al. Precipitation hardening of anAl–4.2 wt% Mg–0.6 wt% Cu alloy. Acta Mater. 1998;46(10):3523–3533.
[34] Feng Z, Yang Y, Huang B, et al. Precipitation process along dislocations in Al–Cu–Mg alloy during artificial aging. Mater Sci Eng A. 2010;528(2):706–714.